Cite this: *INEOS OPEN*, **2025**, *8 (1–3)*, XX–XX
DOI: 10.32931/ioXXXXx

Received XX Month 20XX,
Accepted 5 April 2025

http://ineosopen.org

SYNTHESIS AND INVESTIGATION OF THE TARGETED DRUG DELIVERY SYSTEMS BASED ON BIMETALLIC NANOPARTICLES Au–FeO_x

A. A. Voronova,*[a] A. Yu. Vasil'kov,[a] A. V. Naumkin,[a] T. Batsalova,[b] and B. Dzhambazov[b]

[a] *Nesmeyanov Institute of Organoelement Compounds, Russian Academy of Sciences, ul. Vavilova 28, str. 1, Moscow, 119334 Russia*
[b] *Faculty of Biology, Paisii Hilendarski University of Plovdiv, 4000 Plovdiv, Bulgaria*

Abstract

New targeted drug delivery systems based on bimetallic AuFe nanoparticles and their conjugates with methotrexate were obtained in different media (acetone and toluene) by the metal-vapor synthesis (MVS). The introduction of methotrexate resulted in a reduction of Fe in both media. In the Au 4f spectra, both gold reduction for the toluene medium and oxidation for the acetone medium were observed. An increase in the size of metal nanoparticles in the presence of methotrexate was observed exclusively in acetone. MTT assay revealed high inhibitory potential of the bimetal conjugates in low concentrations.

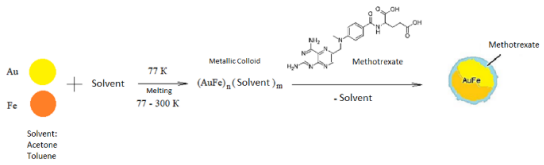

Key words: anticancer drug, AuFe nanoparticles, methotrexate, metal-vapor synthesis, XPS.

Introduction

Chemotherapy, one of the main methods for treating oncological diseases, has a number of limitations due to the fact that the non-specificity of drugs leads to undesirable side effects [1]. Metal nanoparticles (MNPs) have potential to solve the problems associated with these limitations, while their conjugation with antitumor agents may provide significant benefits in cancer therapy. A number of conjugates of MNPs with methotrexate have shown efficiency in the treatment of various types of cancer [2, 3]. New targeted drug delivery systems based on mono- and bimetallic Au, Fe, and AuFe nanoparticles and their conjugates with methotrexate (MTX) were obtained by the metal-vapor synthesis [4, 5].

Results and discussion

The MVS method ensures the production of mono- and bimetallic nanoparticles with different ratios of the components. When gold and iron atoms interact with toluene, organosol Au NPs and a thermolabile bis(toluene)Fe complex, stable at temperatures below –40 °C, are formed (Scheme 1). Then, upon heating to room temperature, colloids of AuFe nanoparticles are formed in toluene (AuFeTol) and acetone (AuFeAc). The analysis of the resulting systems by X-ray photoelectron spectroscopy (XPS) revealed that the use of toluene in the MVS leads to the formation of a state close to FeO. The main Fe $2p_{3/2}$ peak of the AuFeTol sample has the lowest binding energy. There is almost no satellite belonging to a Fe^{3+} state in the spectrum of AuFeTolMTX (Fig. 1). After the modification of the Fe NPs with methotrexate, the intensity of the satellite is significantly reduced, indicating the predominance of a Fe^{2+} state.

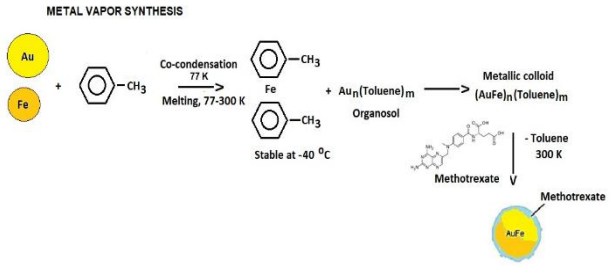

Scheme 1. Synthesis of nanoparticles.

The Au $4f_{7/2}$ peaks of the AuFeAc and AuFeTol samples (Fig. 1) are characterized by a positive chemical shift of 0.3 eV, but feature different values of FWHM (1.02 and 1.44 eV) (see Fig. S1 in the Electronic complementary information (ESI)), which may be due to the nanoscale particle sizes and the presence of Au–O bonds in AuFeTol (Fig. S2 in the ESI). The spectra of AuFeAc and Au foil are almost identical in shape (Fig. S3 in the ESI). The interaction of AuFeAc and AuFeTol with methotrexate leads to a shift in the spectra by –0.3 and 0.45 eV, respectively, with concomitant narrowing and broadening of the peaks, which in the case of AuFeAc may indicate the lack of Au–O bonds and the formation of Au–N bonds, while in the case of AuFeTol it may indicate the formation of Au–O bonds.

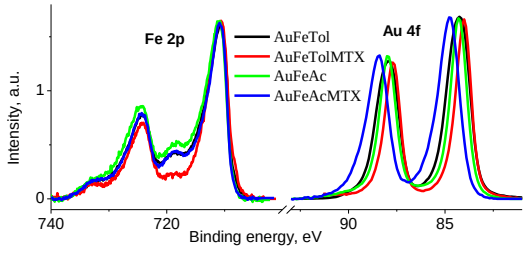

Figure 1. Fe 2p and Au 4f XPS spectra of the samples explored.

The concentrations of the elements on the surface of the samples explored, calculated from the high-resolution XPS spectra, are shown in Table S1 in the ESI.

The size distributions of AuFeAc nanoparticles and their conjugates with methotrexate was studied by small-angle X-ray scattering (SAXS). The initial sections of the SAXS diagrams indicate the presence of large aggregates in the samples (Fig. S4 in the ESI). The bimetallic samples are characterized by the presence of highly homogeneous populations of individual NPs along with a high content of large aggregates. The metallic iron particles contain both small particles with an average radius of about 4.6 nm and aggregates with a radius of up to 45 nm. In the presence of methotrexate, the number of aggregates increases, and the content of small nanoparticles becomes more pronounced. The modification with methotrexate leads to increased interaction between nanoparticles and, as a result, to the formation of larger aggregates in the conjugates.

The experimental scattering curves of the bimetallic nanoparticles of AuFeTol and those modified with methotrexate differ only slightly (Fig. 2). The modification of nanoparticles with this drug does not lead to their additional aggregation. The distribution functions are bimodal and reveal narrow populations of individual MNPs together with a wide fraction of aggregates. The narrow fraction of individual bimetallic nanoparticles consists of nanoparticles with an average radius of $R_{ind} \approx 1$ nm for both samples, while their aggregates reach a size of $R_{agg} = 30$ nm for the initial particles and $R_{agg} = 32$ nm for the nanoparticles modified with methotrexate.

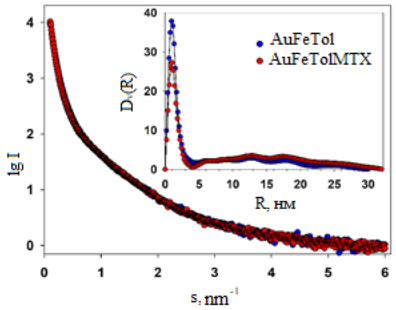

Figure 2. SAXS curves for the bimetals and their conjugates obtained in toluene. Inset: volume size distribution functions $D_V(R)$.

The investigations of the antibacterial activity revealed moderate inhibitory effects of the conjugates against gram-negative and gram-positive bacteria (Table S2 in the ESI). The level of inhibition detected in normal human fibroblasts did not exceed 25% at the highest tested concentrations of the bimetal conjugates. This effect was manifested in the early testing periods of 24 and 48 h, which indicates the ability of cells to overcome cytotoxic effects and a good potential for biocompatibility of the samples (Fig. 3a). In low concentrations (10 μg/mL), the bimetal conjugates display high inhibitory potential against human lung carcinoma cells A549 (Fig. 3b). The conjugate-induced inhibition can be explained by the effective drug targeting and possible synergistic effects.

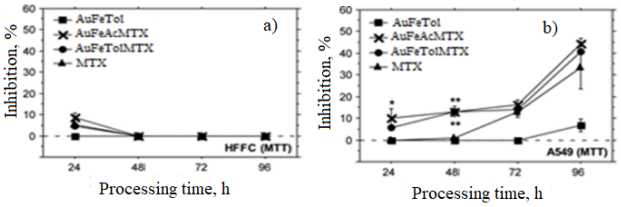

Figure 3. Cytotoxicity of the NPs under consideration against human fibroblasts (***a***) and human lung carcinoma cells (***b***).

Conclusions

The metal-vapor synthesis can be used for the creation of targeted drug delivery systems based on bimetallic AuFe nanoparticles and their conjugates with methotrexate. The resulting materials showed moderate inhibitory activity against gram-negative and gram-positive bacteria. The bimetal conjugates exhibited good biocompatibility potential in *in vitro* assays with normal human fibroblasts. The analyses revealed prominent inhibitory properties of AuFeMTX NPs against human lung carcinoma cells in low concentrations.

Acknowledgements

This work was supported by the Ministry of Science and Higher Education of the Russian Federation (agreement no. 075-00277-24-00).

The authors are grateful to E. Shtykova and V. Volkov for the SAXS studies.

Corresponding author

* E-mail: voronova.anastasiia.a@mail.ru. Tel: +7(999)801-6219 (A. A. Voronova).

Electronic supplementary information

Electronic supplementary information (ESI) available online: the syntheses, XPS and SAXS data, antibacterial activity. For ESI, see DOI: 10.32931/ioXXXXx.

References

1. M. Younis, M. Iqbal, N. Shoukat, B. Nawaz, F. H. Watto, K. A. Shahzad, *Sci. Lett.*, **2014,** *2*, 15–18.
2. Y.-H. Chen, C.-Y. Tsai, P.-Y. Huang, M.-Y. Chang, P.-C. Cheng, C.-H. Chou, D.-H. Chen, C.-R. Wang, A.-L. Shiau, C.-L. Wu, *Mol. Pharmaceutics*, **2007**, *4*, 713–722. DOI: 10.1021/mp060132k
3. T. Kubo, K. Tachibana, T. Naito, S. Mukai, K. Akiyoshi, J. Balachandran, K. Otsuka, *ACS Biomater. Sci. Eng.*, **2019**, *5*, 759–767. DOI: 10.1021/acsbiomaterials.8b01401
4. A. A. Voronova, A. V. Naumkin, A. Yu. Vasil'kov, *INEOS OPEN*, **2022**, *5*, 79–84. DOI: 10.32931/io2215a
5. A. Voronova, A. V. Naumkin, A. Ya. Pereyaslavtsev, T. Batsalova, B. Dzhambazov, A. Vasil'kov, *Dokl. Phys. Chem.*, **2024**, *514*, 1–8. DOI: 10.1134/S0012501624600025